# Fe-MCM-41 for $N_2O$ Decomposition and Reduction with Methane

Yan Tian,[1] Erika Ogawa,[1] Akira Ikuo,[1] Tetsuya Shishido,*[1] Quinghong Zhang,[2] Ye Wang,[2]
Katsuomi Takehira,[3] and Sadao Hasegawa[1]
[1]*Department of Chemistry, Tokyo Gakugei University, 4-1-1 Nukui-kita, Koganei, Tokyo 184-8501*
[2]*State Key Laboratory for Physical Chemistry of Solid Surfaces, Department of Chemistry, Xiamen University, Xiamen 361005, P. R. China*
[3]*Graduate School of Engineering, Hiroshima University, 1-4-1 Kagamiyama, Higashi-hiroshima 739-8527*

(Received January 25, 2006; CL-060109; E-mail: stetsuya@u-gakugei.ac.jp)

The catalytic activities for $N_2O$ decomposition and selective reduction with methane were studied on Fe-MCM-41 prepared by direct hydrothermal synthesis (DHT) and template ion exchange (TIE) methods. Fe-MCM-41-DHT showed higher activity than those prepared by TIE and impregnation methods. The high activity of Fe-MCM-41-DHT is caused by the formation of highly isolated and tetrahedrally coordinated iron-oxo species.

---

Nitrous oxide ($N_2O$) is a strong greenhouse-effect gas with a global warming potential (GWP) per molecule of about 300 times stronger than that of carbon dioxide, and it also affect the destruction of the stratospheric ozone layer.[1] For the catalytic removal of $N_2O$, decomposition and selective reduction (SCR) with reductants have been proposed as effective methods. Many iron-containing catalysts such as ferrisilicate, Fe-ZSM-5, Fe-$\beta$, $Fe/Al_2O_3$, etc. have been reported to catalyze both $N_2O$ decomposition and SCR.[2–4] Particularly, numerous investigations have focused on Fe ion-exchanged zeolites since the first report of Segawa et al. on the high performance of Fe-ZSM-5 for $N_2O$ SCR with $C_3H_6$ in the presence of $H_2O$ and $O_2$.[5,6] Many researchers have pointed out that Fe binuclear species are active sites for $N_2O$ decomposition and SCR.[2,3,7–9] On the other hand, mononuclear iron-oxo species have been also proposed as active sites for $N_2O$ SCR.[5,6,10] Shimokawabe et al. reported that tetrahedrally coordinated $Fe^{3+}$ in ion-exchanged Fe-ZSM-5 showed higher activity in $N_2O$ SCR than small $Fe_2O_3$ cluster in ZSM-5 prepared by impregnation method.[11] Moreover, Joyner and Stockenhuber reported that Fe in Fe/ZSM-5 prepared with different ion-exchange methods was stabilized in different forms, ranging from isolated metal ions to large oxide clusters.[12] They concluded that iron-oxo nanoclusters are most active in the $NO_x$ SCR. Thus, the coordination environments of active iron species for the removal of $N_2O$ are still under discussion. Metal ion-containing mesoporous silicates such as M41S and SBA-15, which possess uniform nano-order mesopores and high concentration of isolated active sites, has attracted much attention as a new type of catalyst. In order to introduce active metal centers to mesoporous silicates, several kinds of methods such as direct hydrothermal, impregnation, grafting, template ion exchange methods,[13] etc. have been proposed. It can be expected that the metal cations with different environments would result in various catalytic properties. Indeed, we recently reported that Fe-MCM-41 prepared by the DHT method is more active than those prepared by TIE and impregnation methods for the epoxidation of styrene with $H_2O_2$.[14] In the present report, we introduce iron species into MCM-41 by DHT and TIE methods. The catalytic performances of Fe-MCM-41 thus prepared were tested in $N_2O$ decomposition and SCR with $CH_4$ and the effects of the coordination environments of iron-oxo species on the catalytic performance are discussed.

Fe-MCM-41 catalysts were prepared by DHT and TIE methods according to the previous report.[14] $Fe_2O_3$/Cab–O–Sil catalyst was also prepared by impregnation method. Cab–O–Sil (Acros Organics Co.) is $SiO_2$, which has no pore structure. The content of iron in each sample was determined by ICP. The catalytic test was carried out using fixed-bed flow reactor. The products were analyzed by on-line TCD gas chromatographs.

Figure 1 represents the temperature dependence of $N_2O$ conversion in the decomposition (A) and SCR with $CH_4$ under an excess of oxygen (B), respectively. $N_2$, $CO_2$, and trace amount of CO were detected in $N_2O$ reduction with $CH_4$. BET surface area, iron content, and TOF values for $N_2O$ decomposition and SCR are shown in Table 1. Although both reactions proceeded over iron-free MCM-41 and Cab–O–Sil above 973 K (not shown), the addition of iron caused an enhancement of $N_2O$ con-

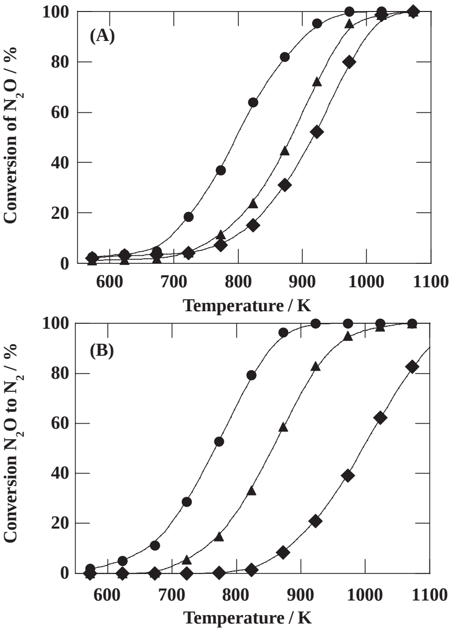

**Figure 1.** Catalytic decomposition of $N_2O$ (A) and selective reduction of $N_2O$ with methane under an excess of oxygen (B), Decomposition: $N_2O$ 1250 ppm, He balance, $W/F = 0.1$ g s mL$^{-1}$, SCR with $CH_4$: $N_2O$ 1250 ppm, $CH_4$ 1250 ppm, $O_2$ 2 vol %, He balance, $W/F = 0.1$ g s mL$^{-1}$; (●) Fe-MCM-41-DHT, (▲) Fe-MCM-41-TIE, (◆) $Fe_2O_3$/Cab–O–Sil.

**Table 1.** Properties and TOF values of iron containing catalysts

| Catalysts | Fe content /wt %[a] | Si/Fe | $S_{BET}$ /m$^2$ g$^{-1}$ | TOF/$\times 10^4$ s$^{-1\,b}$ | |
|---|---|---|---|---|---|
| | | | | Decomp. | SCR |
| DHT | 1.69 | 54 | 1020 | 6.7 | 6.2 |
| TIE | 1.37 | 67 | 738 | 2.8 | 1.3 |
| $Fe_2O_3$/Cab–O–Sil | 1.55 | 59 | 198 | 1.5 | 0.0 |
| MCM-41 | — | — | 1048 | — | — |

[a]Determined by ICP analysis. [b]Reaction temp.; Decomposition: 773 K, SCR with $CH_4$: 723 K.

version at low temperatures. Among the catalyst tested, Fe-MCM-41-DHT clearly showed the highest $N_2O$ conversion in both reactions over the temperature range of 673 to 1073 K. $Fe_2O_3$/Cab–O–Sil showed the lowest $N_2O$ conversion in both reactions. In the case of SCR under excess of oxygen over $Fe_2O_3$/Cab–O–Sil, $CH_4$ conversion was much higher than $N_2O$ conversion, indicating that combustion of $CH_4$ prominently proceeded. TOF values for $N_2O$ decomposition at 773 K and SCR with $CH_4$ at 723 K over Fe-MCM-41-DHT were $6.7 \times 10^{-4}$ and $6.2 \times 10^{-4}$ s$^{-1}$ and these values are ca. 2.4 and 4.8 times larger than those over Fe-MCM-41-TIE, respectively. These results strongly suggest that the coordination environment of iron was crucial for both $N_2O$ decomposition and SCR with methane. The XRD patterns showed that the Fe-MCM-41-DHT and TIE had hexagonal regularity and their pore diameters determined by $N_2$ adsorption were around 2.7 nm. Both Fe-MCM-41-DHT and TIE preserved this hexagonal regularity even after the reaction at 1073 K. Figure 2 shows the diffuse reflectance UV–vis spectra of Fe-MCM-41 along with $Fe_2O_3$/Cab–O–Sil. In the case of Fe-MCM-41-DHT, a sharp peak at 265 nm was obtained. This band was similar to that for ferrisilicate containing tetrahedrally coordinated iron species and could be assigned to the d$\pi$–p$\pi$ charge transfer between the Fe and O atoms in the framework of Fe–O–Si in the zeolite.[15] On the contrary, in the cases of Fe-MCM-41-TIE and $Fe_2O_3$/Cab–O–Sil, bands at ca. 385 and 510 nm were mainly observed. $\alpha$-$Fe_2O_3$ also shows these bands[4] suggesting the formation of $Fe_2O_3$ cluster over Fe-MCM-41-TIE and $Fe_2O_3$/Cab–O–Sil. The pre-peak intensity in XANES spectrum of the Fe-MCM-41-DHT was almost similar to that of ferrisilicate, whereas higher than those of Fe-MCM-41-TIE and $\alpha$-$Fe_2O_3$. This result suggests that the iron species in Fe- MCM-41-DHT and TIE exist in tetrahedrally and octahedrally coordinated environments, respectively. The curve-fitting analysis of Fe K-edge EXAFS are summarized in Table 2. As for the Fe-MCM-41-DHT, the incorporation of the majority of $Fe^{3+}$ into the framework of MCM-41 with a tetrahedral coordination structure is inferred, since both the Fe–O distance (1.85 Å) and the coordination number (4.2) of Fe-MCM-41 were similar to those of the ferrisilicate.[16] On the other hand, two kinds of Fe–O shells with the coordination numbers of 3.2 and 3.2, respectively, were obtained in Fe-MCM-41-TIE. The iron in $\alpha$-$Fe_2O_3$ possessed two kinds of Fe–O shells with the coordination numbers of 3.0 and 2.9, respectively. The coordination number of Fe–Fe shell in Fe-MCM-41-TIE (2.1) was much smaller than that in $\alpha$-$Fe_2O_3$ (7.0).[17] These results suggest that iron in Fe-MCM-41-DHT is highly dispersed and mainly incorporated into the framework of MCM-41. On the other hand, Fe-MCM-41-TIE mainly contains iron oxide clusters, which have octahedrally coordinated Fe species. $Fe_2O_3$/Cab–O–Sil, which was prepared by impregnation method, also contains iron oxide clusters. Therefore, the tetrahedrally coordinated iron-oxo species in Fe-MCM-41-DHT showed high activity in both $N_2O$ decomposition and reduction with methane, whereas the iron oxide clusters in Fe-MCM-41-TIE showed low activity. Moreover, the Fe-MCM-41-DHT showed no decreasing in the activity for $N_2O$ reduction by methane under an excess of oxygen during the reaction for 24 h, suggesting that the tetrahedrally coordinated iron-oxo species in MCM-41 has high stability.

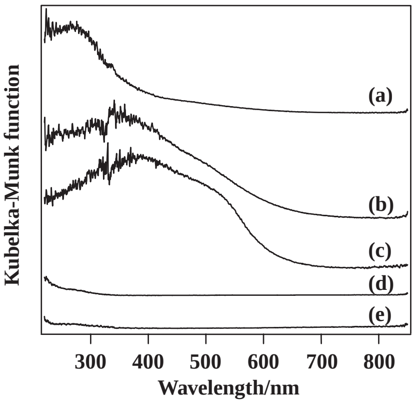

**Figure 2.** UV–vis spectra of iron-containing catalysts, iron-free MCM-41 and Cab–O–Sil. (a) Fe-MCM-41-DHT, (b) Fe-MCM-41-TIE, (c) $Fe_2O_3$/Cab–O–Sil, (d) MCM-41, and (e) Cab–O–Sil.

**Table 2.** Curve-fitting analysis of Fe-MCM-41 and reference compounds

| Samples | Scatter | C.N.[a] | R/Å[b] | DW/$\times 10^3$ Å$^{2\,c}$ |
|---|---|---|---|---|
| Ferrisilicate | O | 3.9 | 1.85 | −0.71 |
| DHT | O | 4.2 | 1.85 | 0.73 |
| TIE | O | 3.2 | 1.85 | −0.73 |
| | O | 3.2 | 1.99 | −0.86 |
| | Fe | 2.1 | 3.06 | 8.93 |
| $\alpha$-$Fe_2O_3$ | O | 3.0 | 1.91 | 0.70 |
| | O | 2.9 | 2.04 | 2.30 |

[a]C.N.: coordination number, [b]R: distance, [c]The difference between the Debye–Waller factors of the samples and reference compounds.

## References

1 H. Rodhe, *Science* **1999**, *248*, 1217.
2 M. Yoshida, T. Nobukawa, S. Ito, K. Tomishige, K. Kunimori, *J. Catal.* **2004**, *223*, 454.
3 S. Kameoka, T. Nobukawa, S. Tanaka, S. Ito, K. Tomishige, K. Kunimori, *Phys. Chem. Chem. Phys.* **2003**, *5*, 3328.
4 M. Haneda, M. Shinriki, Y. Nagao, Y. Kintaichi, H. Hamada, *Bull. Chem. Soc. Jpn.* **2003**, *76*, 2329.
5 C. Pophal, T. Yogo, K. Tanabe, K. Segawa, *Catal. Lett.* **1997**, *44*, 271.
6 K. Yamada, S. Kondo, K. Segawa, *Microporous Mesoporous Mater.* **2000**, *35–36*, 227.
7 A. A. Battiston, J. H. Bitter, F. M. F. de Groot, A. R. Overweg, O. Stephan, J. A. van Bokhoven, P. J. Kooyan, C. van der Spek. G. Vanko, D. C. Koningsberger, *J. Catal.* **2003**, *213*, 251.
8 P. Marturano, L. Drozdová, A. Kogelbauer, R. Prins, *J. Catal.* **2000**, *192*, 236.
9 El-M. El-Malki, R. A. van Santen, W. M. H. Sachtler, *J. Catal.* **2000**, *196*, 212.
10 G. Delahay, M. Mauvezin, B. Coq, S. Kieger, *J. Catal.* **2001**, *202*, 156.
11 M. Shimokawabe, T. Chaki, S. Ozawa, M. Arai, *React. Kinet. Catal. Lett.* **2005**, *86*, 363.
12 R. Joyner, M. Stockenhuber, *J. Phys. Chem. B* **1999**, *103*, 5963.
13 M. Yonemitsu, Y. Tanaka, M. Iwamoto, *J. Catal.* **1998**, *178*, 207.
14 Q. Zhang, Y. Wang, S. Itsuki, T. Shishido, K. Takehira, *Chem. Lett.* **2001**, 946.
15 B. Echchahed, A. Moen, D. Nicholson, L. Bonneviot, *Chem. Mater.* **1997**, *9*, 1716.
16 F. Ray, G. Sanker, T. Maschmeyer, J. M. Thomas, R. G. Bell, *Top. Catal.* **1996**, *3*, 121.
17 S. Wong, J. Lee, S. Chemg, C. Mou, *Appl. Catal., A* **2000**, *198*, 115.

Published on the web (Advance View) May 5, 2006; DOI: 10.1246/cl.2006.544